ISBN: 978-3-95450-247-9 ISSN: 2673-5490 doi: 10.18429/JACoW-IPAC2024-THPC66

CROSSING TRANSITION IN THE EIC HSR WITH A RESONANCE ISLAND JUMP SCHEME

S. Peggs*, A. Drees, H. Lovelace III, G. Robert-Demolaize, BNL, Upton, NY, USA
T. Satogata, TJNAF, Newport News, VA, USA

Abstract

The Resonance Island Jump (RIJ) scheme for transition crossing in the Hadron Storage Ring (HSR) of the Electron-Ion Collider (EIC) is radically new. Beam experiments are necessary in RHIC if the RIJ scheme is to be considered a serious alternative to upgrading the first order linear jump scheme currently implemented in RHIC. The detailed theoretical foundations of the RIJ scheme are summarized, and potential RHIC beam experiments are considered.

INTRODUCTION

Stored beam is usually found on a closed orbit that repeats itself every turn, near the design trajectory at the center of the beam pipe. Small amplitude horizontal motion around that closed orbit is then characterized by the closed orbit displacement and angle, Twiss parameters, tune, chromaticity, and the transition gamma: $x_{CO}, x'_{CO}, \beta_x, \alpha_x, Q_x, \chi_x$, and γ_T.

In a Resonance Island Jump (RIJ) scheme beam is trapped in a horizontal resonance island just before or after transition [1–3]. Closed orbit motion repeats, for example, every $N = 4$ turns, with many octupoles driving the resonance. All trapped particles have a betatron tune of exactly $Q_x = 1/4$ (or 3/4), even if they have a non-zero momentum offset, $\delta = \Delta p/p$. The islands have global parameters: island tune, island chromaticity, and island transition gamma: Q_I, χ_I, and γ_{TI}, where the island chromaticity is

$$\chi_I = \frac{dQ_I}{d\delta} \tag{1}$$

Each island is also characterized by local closed orbit and Twiss parameter values: x_I, x'_I, β_I, and α_I.

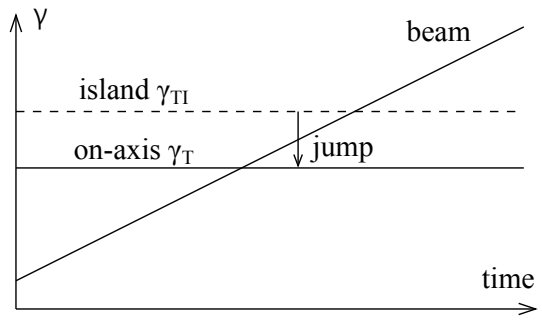

Figure 1: A Resonance Island Jump made as the beam γ accelerates through transition. Here it is assumed that $\gamma_{TI} > \gamma_T$, although the opposite may be true.

* peggs@bnl.gov

A successful RIJ scheme needs

$$\left|\gamma_T - \gamma_{TI}\right| \simeq 1 \tag{2}$$

Figure 1 illustrates a $\gamma_{TI} > \gamma_T$ configuration, in which N islands with identical populations are opened adiabatically before transition [1]. Beam is fast-kicked back on-axis in the same way that the CERN-PS kicks beam over 4 turns into an extraction channel in the Multiturn Resonance Extraction scheme [4–9]. If $\gamma_{TI} < \gamma_T$ then a fast kicker moves all the beam into one island in a single turn at transition, with later adiabatic closure. In both cases an appropriate fast kicker is required. The need for *two* fast kickers is avoided by adiabatically opening or closing the islands.

All three global quantities $(Q_I, \chi_I, \gamma_{TI})$ can be measured in RHIC beam studies, for example during repeated beam stores at injection energy. Beam could be injected directly into a single resonance island, or N equally-populated islands could be adiabatically opened for measurements and observations. The island tune Q_I can be measured using an externally applied tune modulation chirp, in a technique first used in the E778 nonlinear beam dynamics experiment at the Tevatron [10–14]. Trapped beam can be accelerated through transition in RHIC, enabling a direct measurement of γ_{TI}.

ARC CORRECTORS

Table 1 lists parameters of key arc correctors [15]. RHIC uses the quadrupoles in a first order matched transition crossing scheme [16], with fast power supplies that can be modulated to measure island tunes [1], (see below). Octupole correctors are used to detune the lattice, and also to drive fourth order resonances, within integrated strength ranges of

$$\begin{aligned} K3L &= \pm 45.02 \quad \mathrm{m}^{-3} \quad \text{injection} \\ &= \pm\ 4.08 \quad \mathrm{m}^{-3} \quad \text{storage} \end{aligned} \tag{3}$$

at gold injection and storage energies of 10 and 110 GeV/u. The detuning coefficients κ_{xx}, κ_{xy}, and κ_{yy} parameterize

Table 1: Arc corrector parameters [15]. RHIC corrector power supplies are ±50 A bipolar.

Type	Field at 25 mm T	Magnetic length m	Quench current A
Quadrupole	0.067	0.555	190
Octupole	0.017	0.571	198

ISBN: 978-3-95450-247-9 ISSN: 2673-5490 doi: 10.18429/JACoW-IPAC2024-THPC66

Table 2: Detuning coefficients in RHIC and HSR [1].

Accel.	Energy /optics	Detuning ranges κ_{xx} $10^3\mathrm{m}^{-1}$	κ_{xy} $10^3\mathrm{m}^{-1}$	κ_{yy} $10^3\mathrm{m}^{-1}$
RHIC	injection	±94.9	±84.2	±92.3
	storage	±9.3	±8.1	±8.8
HSR	injection	±179.1	±207.8	±287.5
	storage	±19.7	±24.0	±29.4

how the horizontal and vertical tunes depend on the horizontal and vertical actions, through

$$\begin{aligned} Q_x(J_x,J_y) &= Q_{x0} + \kappa_{xx}J_x + \kappa_{xy}J_y \\ Q_y(J_x,J_y) &= Q_{y0} + \kappa_{xy}J_x + \kappa_{yy}J_y \end{aligned} \quad (4)$$

with extreme values listed in Table 2 in octupole-dominated optics [1].

ISLAND MANIPULATION

The general four-turn Kobayashi Hamiltonian [17] in horizontal action angle space (J,ψ) is

$$H_4(J,\psi) = 2\pi\Delta Q\, J + V_{40}\, J^2 + V_{44}\, J^2 \sin(4\psi+\psi_{444}) \quad (5)$$

where the tune separation

$$\Delta Q = Q_0 - \frac{M}{4} \quad (6)$$

is small, and the net motion over four turns

$$\begin{aligned} \Delta\psi &\approx 4\,\frac{\partial H_4}{\partial J} \\ \Delta J &\approx -4\,\frac{\partial H_4}{\partial \psi} \end{aligned} \quad (7)$$

depends on control parameters $V_{40}, V_{44}, \psi_{444}$ given by

$$\begin{aligned} V_{40} &= \pi\kappa_{xx} = \frac{1}{16}\sum_{\mathrm{ps}} K3L \left(\sum_{\mathrm{oct}} \beta^2\right) \\ \vec{V}_{44} &= V_{44}\begin{pmatrix} \sin(\psi_{444}) \\ \cos(\psi_{444}) \end{pmatrix} = \sum_{\mathrm{ps}} K3L\ \vec{S}_{PS} \end{aligned} \quad (8)$$

with double sums over octupoles and their families. Octupoles control the detuning scalar V_{40} as well as the resonance driving vector $\vec{V}_{44}$.

The resonance driving sensitivity vectors are

$$\vec{S}_{PS} = \sum_{\mathrm{oct}} \frac{-\beta^2}{48}\begin{pmatrix} \sin(4\theta-\pi/2) \\ \cos(4\theta-\pi/2) \end{pmatrix} \quad (9)$$

for each of the 24 power supplies, where θ is the horizontal betatron phase of each octupole in that family [1]. Figure 2 shows sensitivity vectors in black for all 12 F-octupole families, and in red for 3 'effective' power supplies formed by adding pairs of F-octupole vectors ($\overrightarrow{bo2} + \overrightarrow{bi8}$, et cetera).

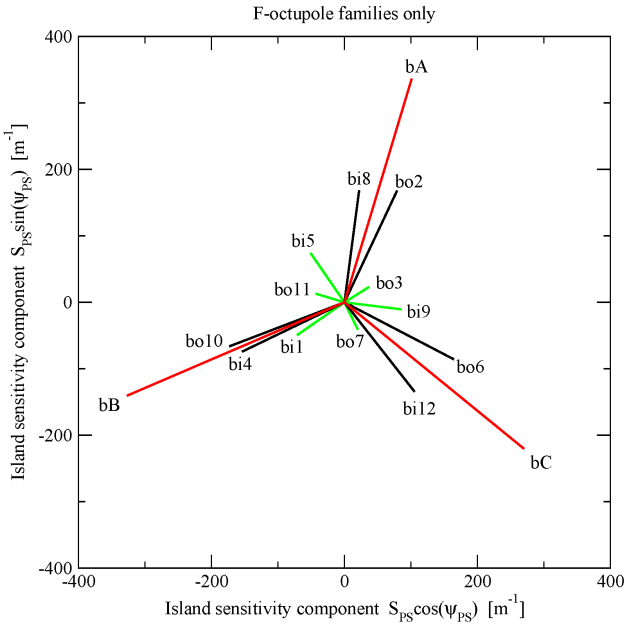

Figure 2: Resonance driving sensitivity vectors $\vec{S}_{PS}$ for the 12 F-octupole families, and the 'effective' power supplies bA, bB, and bC.

Table 3: Sensitivity vectors $\vec{S}_{PS}$ for bA, bB, and bC.

Family	Sensitivity vector $\vec{S}_{PS}$ S_{PS} m^{-1}	ψ_{PS} rad
bA	351.5	1.2786
bB	356.0	3.5473
bC	348.4	5.5989

The angles of the $\overrightarrow{bA}$, $\overrightarrow{bB}$, and $\overrightarrow{bC}$ vectors differ by about 120 degrees, so all net phases are accessible by powering just these 3 logical families, within maximum ranges given by Table 3 and Eq. (3).

The action J_{FP} of the stable fixed point at the heart of a resonance island

$$J_{FP} = -\frac{\pi}{V_{40}}\Delta Q \quad (10)$$

is positive (and physical) only if ΔQ has the correct sign. The island action half-width is

$$I_{HW} = \pi\left|\frac{2V_{44}}{V_{40}^3}\right|^{1/2}|\Delta Q| \quad (11)$$

and the island tune for small oscillations at the island center is

$$Q_I = \left|\frac{8\,V_{44}}{V_{40}}\right|^{1/2}|\Delta Q| \quad (12)$$

Equations 11 and 12 show that at fixed ΔQ the island is strengthened with larger driving strength V_{44}, but is weakened with larger detuning V_{40}.

ISBN: 978-3-95450-247-9 ISSN: 2673-5490 doi: 10.18429/JACoW-IPAC2024-THPC66

MEASURING ISLAND PROPERTIES

The island transition γ_{TI} can be measured by observing when longitudinal stability is lost (with no RF phase jump) as beam is accelerated. Island chromaticity χ_I is found by measuring γ_{TI} at multiple values of δ. The island tune Q_I can be measured by imposing a controlled tune modulation

$$Q_0 \;=\; Q_{00} \;+\; q\,\sin(2\pi\,Q_M t) \tag{13}$$

on beam trapped in a resonance island, where t is turn number and q and Q_M are tune modulation amplitude and tune. For example, the persistent signal initially visible on beam position monitors is lost when a low amplitude chirp from A to B in Fig. 3 crosses the narrow region of chaos near $Q_M = Q_I$ [13, 14].

Three boundaries separate four dynamical partitions in tune modulation space, as shown in Fig. 3:

$$\begin{aligned}
\left(\frac{q}{Q_I}\right) \quad \left(\frac{Q_M}{Q_I}\right) \quad &= \quad \frac{1}{N} \\
\left(\frac{q}{Q_I}\right) \quad \left(\frac{Q_M}{Q_I}\right)^{-1} \quad &= \quad \frac{1}{N} \\
\left(\frac{q}{Q_I}\right)^{1/4} \left(\frac{Q_M}{Q_I}\right)^{3/4} \quad &= \quad \frac{4}{(N\pi)^{1/4}}
\end{aligned} \tag{14}$$

Numerical and beam studies broadly confirm the locations of these four partitions, with boundaries that apply no matter what the resonance source (beam-beam or magnetic), or the tune modulation source (chromatic or external). Their universality emphasizes the crucial role played by the island tune, Q_I. Numerical studies also show a significant amount of additional fine structure, seen at the bottom of Fig. 3 [1, 14].

Tune modulation can be driven by repurposing the RHIC transition jump quadrupoles. At gold injection energy an AC current I_{AC} delivers an amplitude of

$$q \;\approx\; 0.0058\,.\,I_{AC}\;[\mathrm{A}] \tag{15}$$

Useful tune modulation amplitudes of order $q \sim 0.01$ only require a current I_{AC} of a couple of amps, where

$$I \;=\; I_{DC} \;+\; I_{AC}\,\sin(2\pi f t) \tag{16}$$

Frequencies as high as $f = 100$ Hz are desirable.

CONCLUSION

An RIJ scheme would exploit a large value of $|\gamma_T - \gamma_{TI}|$ by using a fast kicker to move beam quickly from closed orbit to island, or vice versa. A simple RHIC experiment would trap beam by adiabatically opening or closing islands, with or without an energy ramp. Octupole power supplies are naturally combined into 3 convenient 'effective' power supplies, bA, bB and bC. Near-resonant horizontal motion is described by a 4-turn Kobayashi Hamiltonian $H_4(J, \psi)$.

Tune modulation enables measurement of Q_I, the sole variable determining 3 universal partition boundaries in tune modulation space. The loss of the persistent signal generated by beam trapped in a resonance island is observed when chirping across a partition boundary. Simulations generally confirm the theoretically predicted partition boundary locations, but also show fine structure that is ripe for further study.

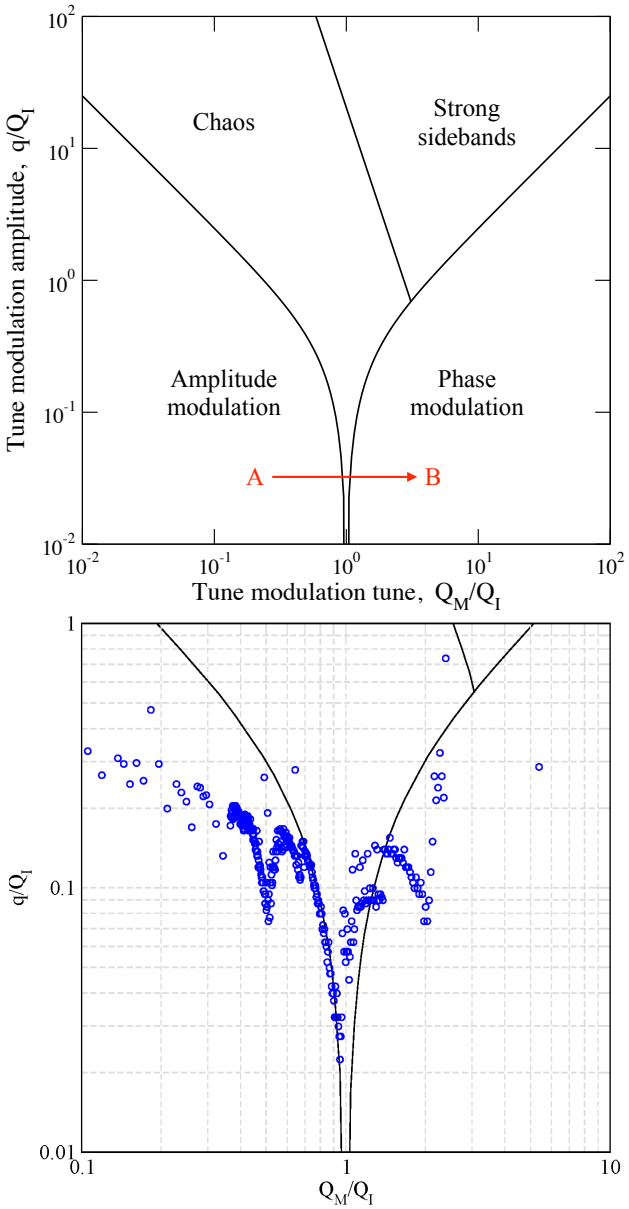

Figure 3: Partitions in tune modulation parameter space for an $N = 4$ resonance.
Top: A chirp from A to B measures island tune Q_I [10].
Bottom: Fine structure found by simulation [1].

ACKNOWLEDGMENTS

Many thanks go to Massimo Giovanozzi, for his encouragement and advice.

ISBN: 978-3-95450-247-9 ISSN: 2673-5490 doi: 10.18429/JACoW-IPAC2024-THPC66

REFERENCES

[1] S. Peggs, H. Lovelace III, G. Robert-Demolaize, and A. Drees, "Resonance island jump theory for the HSR", BNL, Upton, NY, USA, Rep. EIC-ADD-TN-077, 2023.

[2] S. Peggs, H. Lovelace III, G. Robert-Demolaize, and A. Drees, "HSR transition jump optics in the September 2022 layout", BNL, Upton, USA, Rep. EIC-ADD-TN-41, 2023.

[3] M. Giovannozzi, L.Huang, A. Huschauer, and A. Franchi, "A novel non-adiabatic approach to transition crossing in a circular hadron accelerator", *Eur. Phys. J. Plus.*, vol. 136, p. 1189, 2021.

[4] M. Giovanozzi *et al.*, "The CERN PS multi-turn extraction based on beam splitting in stable islands of transverse phase space", CERN, Geneva, Switzerland, Rep. CERN-2006-011, 2006.

[5] S. Gilardoni *at al.*, "Experimental evidence of adiabatic splitting of charged particle beams using stable islands of transverse phase space", *Phys. Rev. Spec. Top. Accel. Beams*, vol. 9, p. 104001, 2006.

[6] A. Franchi, S. Gilardoni, and M. Giovannozzi, *Phys. Rev. Spec. Top. Accel. Beams*, vol. 12, p. 014001, 2009.

[7] E. Benedetto *et al.*, "Results from the 2009 beam commissioning of the CERN multi-turn extraction", in *Proc. IPAC'10*, Kyoto, Japan, May 2010, paper THOBMH02, pp. 3619–3621.

[8] A. Bazzani, C. Frye, M. Giovannozzi, and C. Hernalsteens, *Phys. Rev. E.*, vol. 89, p. 042915, 2014.

[9] J. Borburgh *et al.*, "First implementation of transversely split proton beams in the CERN Proton Synchrotron for the fixed-target physics programme", *Europhys. Lett.*, vol. 113, no. 3, p. 34001, 2016.

[10] S. Peggs, "Hamiltonian theory of the E778 nonlinear dynamics experiment", Rep. SSC-175; CERN 88-04; ICFA Lugano workshop, 1988.

[11] L. Merminga *et al.*, "Nonlinear dynamics experiment in the Tevatron", *Proc. PAC 89*, Chicago, IL, USA, Mar. 1989, pp. 1429–1432.

[12] A. Chao *et al.*, "Experimental investigation of nonlinear dynamics in the Fermilab Tevatron", *Phys. Rev. Lett.*, vol. 61, no. 24, p. 2752, 1988.

[13] T. Satogata *et al.*, "Driven response of a trapped particle beam", *Phys. Rev. Lett.*, vol. 68, no. 12, p. 1838, 1992.

[14] T. Satogata, "Nonlinear resonance islands and modulational effects in a proton synchrotron", Ph.D. thesis, Physics Department, Northwestern University, Chicago, 1993.

[15] " RHIC configuration manual", Table 7-3, p 59., BNL, Upton, NY, USA, Rep. EIC-ADD-TN-56, 2006.

[16] "The RHIC accelerator", *Annu. Rev. Nucl. Part. Sci.*, vol. 52, pp. 245–269, 2002.

[17] Y. Kobayashi, "Theory of the resonant beam ejection from synchrotrons", *Nucl. Instrum. Methods*, vol. 83, pp. 77–80, 1970.